

Efficient Estimation of Barycentered Relative Time Delays for Distant Gravitational Wave Sources

Orion Sauter,^{1,*} Vladimir Dergachev,^{2,3,†} and Keith Riles^{1,‡}

¹*University of Michigan, 450 Church Street, Ann Arbor, Michigan 48109, USA*

²*Max Planck Institute for Gravitational Physics (Albert Einstein Institute), Callinstraße 38, 30167 Hannover, Germany*

³*Leibniz Universität Hannover, D-30167 Hannover, Germany*

Accurate determination of gravitational wave source parameters relies on transforming between the source and detector frames. All-sky searches for continuous wave sources are computationally expensive, in part, because of barycentering transformation of time delays to a solar system frame. This expense is exacerbated by the complicated modulation induced in signal templates. We investigate approximations for determining time delays of signals received by a gravitational wave detector with respect to the solar system barycenter. A highly non-linear conventional computation is transformed into one that has a pure linear sum in its innermost loop. We discuss application of these results to determination of the maximal useful coherence length of continuous wave searches.

Keywords: LIGO; Gravitational Waves; Solar System Modeling

I. INTRODUCTION

The hunt for the first detection of continuous gravitational waves (CW) is under way with many searches published[1–7, 9, 10, 12–23, 26, 27, 29–32, 40] or in progress. Some searches target known sources, such as the Crab Pulsar, but other all-sky searches look for unknown sources over a broad frequency band. These searches require substantial computational resources, so any reduction in computational demands is helpful. In this paper, we examine one aspect of the searches amenable to simplification: calculation of signal time delays received by a gravitational wave detector with respect to the solar system barycenter for an ensemble of assumed source sky positions¹.

The LIGO Analysis Library[38] (LAL) used in many gravitational wave searches includes two methods used to orient detectors, signals, and sources in space and time: *LALBarycenterEarth* gives the Earth’s position in the International Celestial Reference Frame[37] (equivalent to J2000), with respect to the Solar System Barycenter. *LALBarycenter* locates the detectors on Earth, and calculates the time a received signal would have been emitted by a wave source given the signal detection time and the source’s direction and distance, and taking into account effects such as Shapiro and Roemer Delays. These programs[11] have been checked by comparison with the widely used radio astronomy timing package, TEMPO2[35, 36].

The Loosely Coherent algorithms [33, 34] used in recent CW searches[8, 24, 28] are constructed to process bunches of nearby signal templates. These bunches form a manifold, the geometry of which influences the effi-

ciency of the algorithm and, of course, its technical implementation. Because corrections from the transition to barycentric time act on phase, the templates have a strong dependence on sky position.

To understand the geometry of the manifold we investigate approximate models for time delays, characterized here by “emission time”, the inferred time of signal emission in the solar system barycenter frame for a given signal reception time at the detector and distance to the source. In addition, our semi-analytic formula provides an efficient way to compute sets of barycentric corrections for nearby templates using piece-wise polynomial approximations.

The analysis of barycenter timing corrections for the Earth-Sun system serves in addition as a model for a general circularized binary with small modulation depth. As the modulations of source and detector add independently, such an analysis could, in principle, be applied to a binary source simply by doubling the number of terms for an assumed signal model.

II. MATHEMATICAL MODEL

The emission time T is a function of detector local time t , source location u and intrinsic source parameters p (for a source in motion). Because modern computer architectures are vector-based, it is typically more efficient to compute arrays of values of $T(t, u, p)$ for sets of times $\mathcal{T} = \{t_i\}$ and templates $S = \{(u_j, p_j)\}$.

For a single template (u_0, p_0) the function $T(t, u_0, p_0)$ has a very non-trivial behaviour due to several nearly periodic influences from the Sun, planets, and the Moon as well as contributions from General Relativity.

Because any analysis method must overlap templates (u, p) closely enough to provide sufficient detection coverage, we can expect to compute arrays $T(\mathcal{T}, u, p)$ for nearby (u, p) .

Therefore, we separate the problem into two parts:

* osauter@umich.edu

† vladimir.ergachev@aei.mpg.de

‡ kriles@umich.edu

¹ See ref. [39] for a recent study exploiting reduced order modeling of barycentering for a targeted search of a single sky location

- Computation of $T(\mathcal{T}, u_0, p_0)$ for a fixed template (u_0, p_0) .
- Computation of differences $\Delta(\mathcal{T}, u, p; u_0, p_0) = T(\mathcal{T}, u, p) - T(\mathcal{T}, u_0, p_0)$

When sets \mathcal{T} and S are finite we know that there exists the following decomposition:

$$\Delta(t_i, u_j, p_j) = \sum_{k=1}^N f_k(t_i) g_k(u_j, p_j) \quad (1)$$

where $f_k(t_i)$ and $g_k(u_j, p_j)$ are, in general, arbitrary single-valued functions.

The key to our approach is that it is possible to find an approximate version of Equation 1 with a number of terms N much smaller than the dimensionality of space spanned by $\Delta(t_i, u_j, p_j)$.

Besides providing computational efficiency this analysis identifies analytical functions f_k and g_k , paving the way for developing advanced *Loosely Coherent* [33, 34] semi-analytic statistics.

III. PRACTICAL IMPLEMENTATION

We describe sky mismatch using small rotations along right ascension and small offsets in declination. The latter is not a rotation but a flow from one equatorial pole to another, symmetrical with respect to Earth rotation. A small region near the source and sink is excised from the grids.

1. Pick a set of signal arrival times \mathcal{T} .
2. Construct a *coarse* sky grid G_t with minimum point separation of ϵ in spherical distance. Add to these grid of points in a neighborhood B_\odot around the Sun's position at each time $t \in \mathcal{T}$.
3. For every time $t \in \mathcal{T}$ and every point in the coarse sky grid G_t , compute the emission times $t_e \in T(t, G_t)$, where T is a function defined in LALBarycenter, returning a vector of emission times corresponding to each arrival time and source location.
4. Introduce a *displacement* grid ΔG of small sky rotations.
5. Compute emission times $T(t, G_{t,r})$ for each grid $G_{t,r}$ displaced by rotation $r \in \Delta G$.
6. Compute the difference $\Delta(t, G_t, r) \equiv T(t, G_{t,r}) - T(t, G_{t,0})$ in emission times for each rotated and unrotated point at each time.
7. Define a function $\tilde{\Delta}(t, G_t, r) \equiv \sum_k a_k x_k$ with a set of coefficients $\{a_k\}$ for parameters $\{x_k\}$, and use least-squares fitting to compute $\{a_k\}$. Ideally, we would want to find $\{a_k\}$ such that $\max(|\tilde{\Delta}(t, G_t, r) - \Delta(t, G_t, r)|)$ is minimized, but the computational costs of such a search are too high.

IV. EXAMPLE

The parameters used in this study are listed in Table I.

We use terms falling into several categories

- Direction-independent terms depending on GPS time and shift in sky position
- Direction differential-independent terms depending on source sky position and GPS time
- Time-independent terms depending on source sky position and shift in position

A. Definitions of Variables

The sky position variables are defined as

$$\begin{aligned} e_1 &= \cos(\delta) \cos(\alpha) \\ e_2 &= \cos(\delta) \sin(\alpha) \\ e_3 &= \sin(\delta) \end{aligned} \quad (2)$$

with $\alpha \in [-\pi, \pi]$ and $\delta \in [-\frac{\pi}{2} + 0.01, \frac{\pi}{2} - 0.01]$. The adjustment by 0.01 radians prevents flow over the poles, which would lead to ambiguous right ascension. The change in e_i for a shift in right ascension $\Delta\alpha$, and in declination $\Delta\delta$ can be approximated via Taylor expansion:

$$\begin{aligned} \Delta e_1 &= (-\frac{1}{2}\Delta\alpha^2 \cos\alpha \cos\delta - \frac{1}{2}\Delta\delta^2 \cos\alpha \cos\delta \\ &\quad + \frac{1}{4}\Delta\alpha^2 \Delta\delta^2 \cos\alpha \cos\delta - \Delta\alpha \cos\delta \sin\alpha \\ &\quad + \frac{1}{2}\Delta\alpha \Delta\delta^2 \cos\delta \sin\alpha - \Delta\delta \cos\alpha \sin\delta \\ &\quad + \frac{1}{2}\Delta\alpha^2 \Delta\delta \cos\alpha \sin\delta + \Delta\alpha \Delta\delta \sin\alpha \sin\delta) \\ \Delta e_2 &= (\Delta\alpha \cos\alpha \cos\delta - \frac{1}{2}\Delta\alpha \Delta\delta^2 \cos\alpha \cos\delta \\ &\quad - \frac{1}{2}\Delta\alpha^2 \cos\delta \sin\alpha - \frac{1}{2}\Delta\delta^2 \cos\delta \sin\alpha \\ &\quad + \frac{1}{4}\Delta\alpha^2 \Delta\delta^2 \cos\delta \sin\alpha - \Delta\alpha \Delta\delta \cos\alpha \sin\delta \\ &\quad - \Delta\delta \sin\alpha \sin\delta + \frac{1}{2}\Delta\alpha^2 \Delta\delta \sin\alpha \sin\delta) \\ \Delta e_3 &= (\Delta\delta \cos\delta - \frac{1}{2}\Delta\delta^2 \sin\delta) \end{aligned} \quad (3)$$

The LALBarycenter program provides vectors with information on the state of the Sun and Earth that are useful:

$$\begin{aligned} \vec{s} &\text{ Vector pointing from Sun to Earth} \\ \vec{v} &\text{ Detector velocity vector} \\ \Delta t &\text{ Time since reference point} \\ \Omega_\oplus &2\pi/\text{sidereal day.} \end{aligned} \quad (4)$$

We also define an array of the sin/cos of the reference point's right ascension and declination:

$$\mathbf{z} = \{\sin\alpha, \sin\delta, \cos\alpha, \cos\delta\} \quad (5)$$

and the second-order terms, excepting \sin^2 terms because they can be expressed as $1 - \cos^2$:

$$\begin{aligned} \mathbf{z}' &= \{\cos^2\alpha, \cos^2\delta, \sin\alpha \sin\delta, \sin\alpha \cos\alpha, \\ &\quad \sin\alpha \cos\delta, \sin\delta \cos\alpha, \sin\delta \cos\delta, \cos\alpha \cos\delta\} \end{aligned} \quad (6)$$

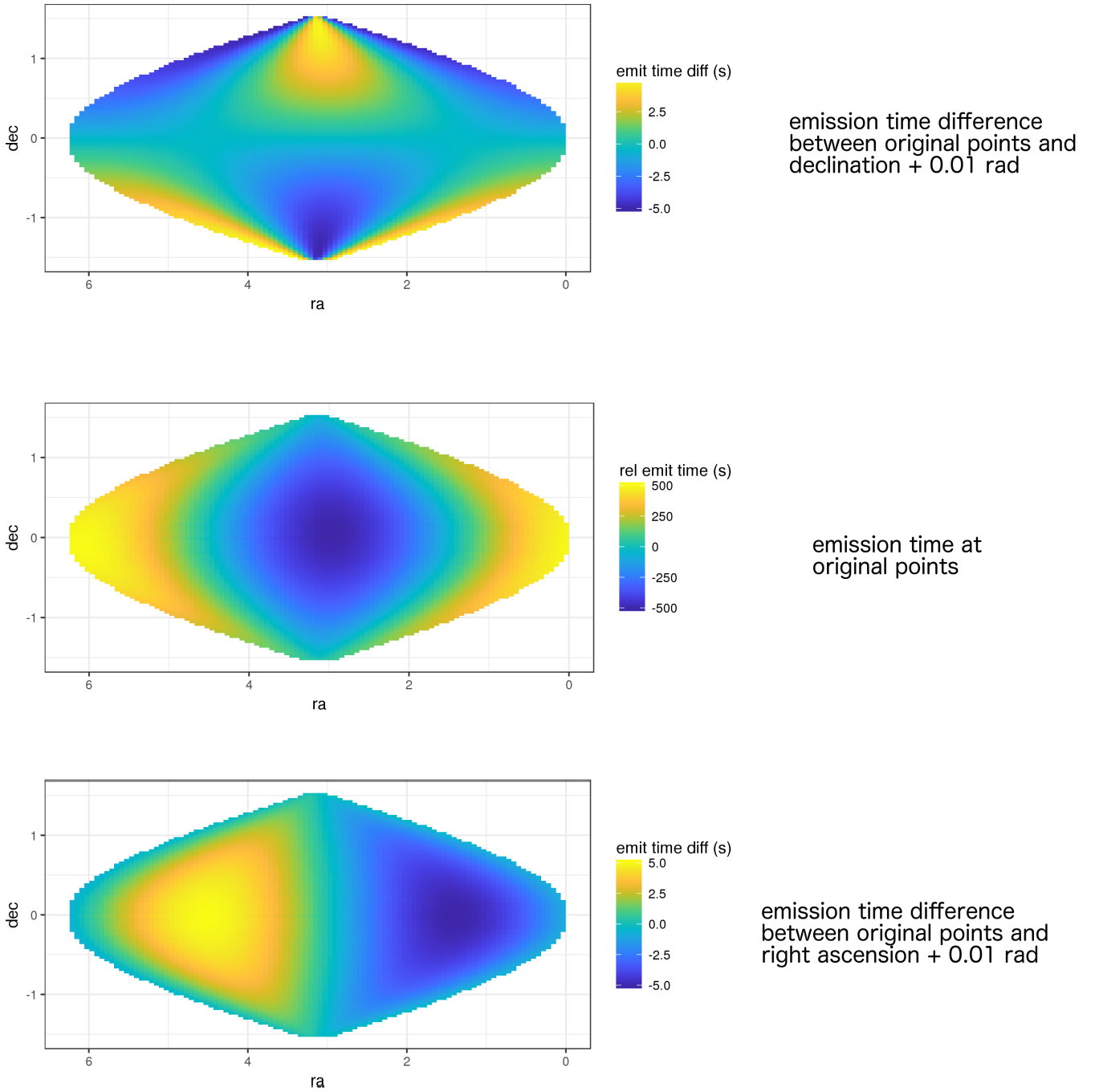


FIG. 1. Example of emission time variation with sky position. The middle panel shows differences between computed emission time and a reference time. The top panel shows differences in emission times between points offset in declination by 0.01 rad, while the bottom panel shows differences in emission times between points offset in right ascension by 0.01 rad. Note that the color scales for difference plots are greatly reduced.

B. Direction-independent terms

The following terms are constant in sky-direction, and can be precomputed for every GPS time, and direction difference.

$$\sum_i a_{1,i} \Delta e_i \quad (7)$$

TABLE I. Parameters used in fits

Parameter	Value
\mathcal{T}	Every hour between t_{\min} and t_{\max}
t_{\min}	From start to end of O1, spaced every 200,000 seconds
t_{\max}	$t_{\min} + 250,000$ sec
ϵ	0.1040524 rad
ΔG	All combinations of $\Delta\alpha$ and $\Delta\delta$
$G_{t,r}$	Random subset of G_t with 7.5×10^5 points
$\Delta\alpha$	$\{-0.01, -0.00667, -0.00333, 0, 0.00333, 0.00667, 0.01\}$
$\Delta\delta$	$\{-0.01, -0.00667, -0.00333, 0, 0.00333, 0.00667, 0.01\}$
ϵ_{\odot}	0.001 rad
N_{\odot}	5
$\mathcal{S}(t)$	Sun position at time t
B_{\odot}	A grid of $N_{\odot} \times N_{\odot}$ points centered on $\mathcal{S}(t)$, evenly spaced in α and δ with step ϵ_{\odot}

C. Difference-independent terms

The following terms are constant in direction-difference.

$$\sum_i a_{2,i} \sin(\Omega_{\oplus} \Delta t) z'_i + b_{2,i} \sin(\Omega_{\oplus} \Delta t) z'_i \quad (8)$$

$$a_{3,1} \Delta t \cos \delta + a_{3,2} \Delta t^2 \cos \delta + a_{3,3} \Delta t \cos^2 \delta \quad (9)$$

$$\sum_i a_{4,i} \Delta t^2 z'_i \quad (10)$$

$$\sum_i a_{5,i} \mathcal{S}_i e_i \quad (11)$$

D. Time-independent terms

The following terms vary only in sky-direction.

$$\sum_i a_{6,i} z_i \quad (12)$$

$$\sum_i a_{7,i} z'_i \quad (13)$$

Each of the terms in equations 7-13 is multiplied by $\Delta\alpha, \Delta\delta, \Delta\alpha^2, \Delta\delta^2, \Delta\alpha\Delta\delta$. In addition, we include direction-time differential terms

$$\sum_i a_{8,i} \Delta t \Delta e_i \quad (14)$$

without $\Delta\alpha/\Delta\delta$ factors. Each term goes to zero when the rotation angle goes to zero. Note that Sun-Earth and detector velocity vectors are those for the saved points. In each term, any parts greater than order 3 in $\Delta\alpha$ and

TABLE II. Term significance analysis. The max error column shows errors when the specified terms are omitted.

Term Group	Equation	Max Fit Error (s)
2nd Order Sinusoids	13	3.4319967642
1st Order Sinusoids	12	0.4335595581
Δt	9	0.0235629364
Δt^2	10	0.0010017764
Sun Direction	11	0.0002486640
Sidereal Rotation	8	0.0001820357
Direction-difference	7	0.0001655650

$\Delta\delta$ are removed. The effects of removing sets of terms are shown in Table II.

An example fit is included in the [appendix](#). This fit has the largest maximum error among the fits, 2.03×10^{-5} s. The fit expression is a bilinear product of precomputed fit coefficients and monomials in $\Delta\alpha$, $\Delta\delta$ and Δt . In a practical implementation the grid of displacements, and thus monomial coefficients, is kept static inside the loop that computes Δt . The actual computation of Δt easily vectorizes and takes few instructions on modern computers. Note that it is not necessary to keep the grid static with respect to all variables. For example, the grid can be static in $\Delta\delta$ and depend on t and α — the monomial grid recompute cost will be amortized away.

V. RESULTS

As a maximum acceptable error, we chose a 30-degree phase difference for a 2 kHz signal, or $42 \mu\text{s}$. The fit terms given above achieved this goal in the fitting set, but we wished to test situations similar to those in which the model would be used. We chose $16 \times 8 = 128$ points on the sky, evenly spaced in right ascension and declination,

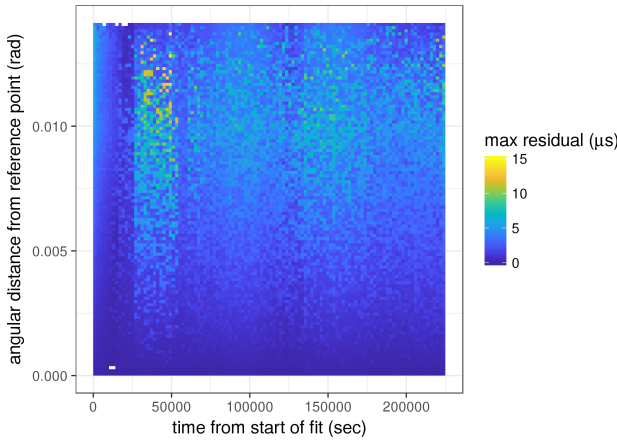


FIG. 2. Maximum absolute residual over all test patches.

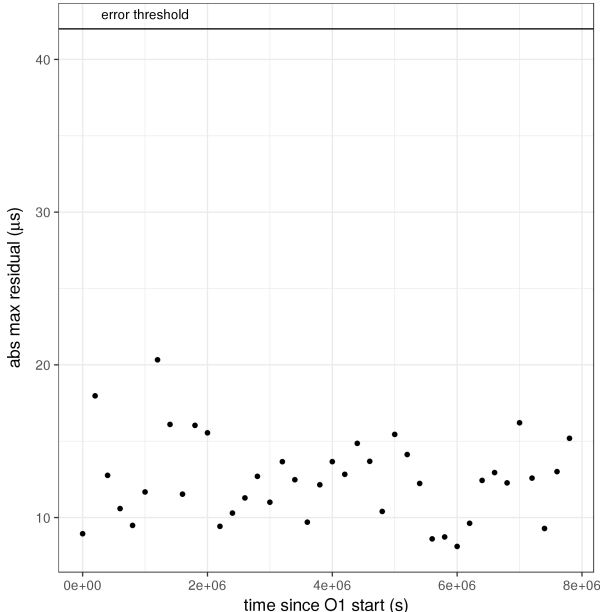


FIG. 3. Maximum absolute residual for each fit.

to serve as patch centers. For each patch, we shifted the central point by a random value in $[-0.01, 0.01]$ for right ascension, and another for declination. A total of 50 shifted points were generated for each patch.

We divided the span of the first Advanced LIGO data run (~ 4 months), O1, into 200,000 second chunks, and took time points from each chunk at 30-minute intervals. We used LALBarycenter to obtain reference values for all points, then applied the fit model to each patch's points as a deflection from its center.

A plot of the maximum absolute residual for each Δt and $\Delta\phi$ is shown in Figure 2. The maximum absolute residual for each reference time is shown in Figure 3. All points fell below the error threshold. We also show a histogram of all errors in Figure 4. The bulk of the errors are well below the threshold, and for a search of this length, any particular point would spend only a small

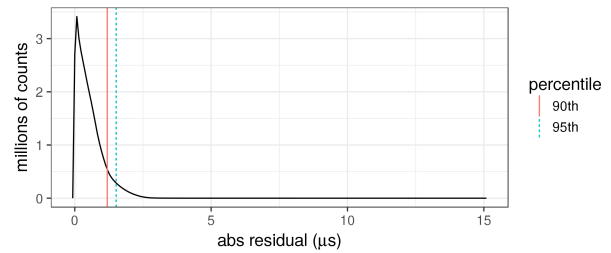


FIG. 4. Distribution of residual magnitude. For large-timebase searches, only the bulk of the distribution matters, which is well below the error threshold.

fraction of time in a high-error region.

VI. CONCLUSIONS

The *Loosely Coherent* method of detecting signals analyzes sets of potential templates. For the set based on nearby sky locations it is important to understand the evolution of signal phases for nearby templates. The fit described in this paper explicitly demonstrates that relatively few parameters are needed to describe time arrival differences between nearby templates.

It is well-known that mathematically optimal detection statistic consists of a linear filter followed by a power detector [41]. The linear filter is chosen to match expected signal properties and to reject noise outside of signal bandwidth. As the [example](#) shows, the sky position mismatch is equivalent to frequency modulation of the incoming signal. Thus for any search where sky position uncertainty requires multiple templates, the fully coherent search is not the most computationally efficient [33] and it is best to compute the total power of the modulated signal.

For example, if such a search uses one year's worth of data from a single interferometer, the maximal sensitivity is reached at 6 months coherence length, or even earlier if parameters other than sky position are uncertain. For a search using many interferometers a fully coherent search can be more sensitive, but the gain in sensitivity is smaller than predicted from the increase of coherence time alone.

This development provides an efficient method to compute emission time corrections, provides a basis for extension of the PowerFlux cache to longer coherence times and lays the groundwork for future development of *Loosely Coherent* algorithms.

VII. ACKNOWLEDGEMENTS

We thank members of the Continuous Waves Search Group of the LIGO Scientific Collaboration and Virgo Collaboration for useful discussions. This work was

partly funded by National Science Foundation grant NSF

PHY 1505932.

Appendix: Example Fit

As an example, we list below the resulting formula from a fit for GPS time 1127833121. The expression is a bilinear product between precomputed fit coefficients and monomials in $\Delta\alpha$, $\Delta\delta$ and Δt . Only significant terms are shown. This fit has the largest maximum error among the fits, 2.03×10^{-5} s.

$$\begin{aligned} \Delta T = & [-1.69]10^{-5}\Delta t\Delta e_1 + [8.98]10^{-5}\Delta t\Delta e_2 + [-495e_2 + 71.2e_1]\Delta\alpha + \\ & [30.8\cos(\delta) - 71.2e_3\sin(\alpha) - 495e_3\cos(\alpha)]\Delta\delta + [3.89\cos(\delta)]10^{-5}\Delta\delta\Delta t + [8.14e_2 + 83e_1]\Delta\alpha^2 + \\ & [0.0132e_2 - 0.00634e_1]\sin(\Omega_{\oplus}\Delta t)\Delta\alpha + [0.00644e_2 + 0.0132e_1]\cos(\Omega_{\oplus}\Delta t)\Delta\alpha + \\ & [-35.6e_2 - 248e_1 - 0.5e_3\mathcal{S}_3]\Delta\delta^2 + [0.00634e_3\sin(\alpha) + 0.0132e_3\cos(\alpha)]\sin(\Omega_{\oplus}\Delta t)\Delta\delta + \\ & [0.0972e_2 - 0.0157e_1]10^{-10}\Delta\alpha\Delta t^2 + [-0.0132e_3\sin(\alpha) + 0.00644e_3\cos(\alpha)]\cos(\Omega_{\oplus}\Delta t)\Delta\delta + \\ & [-0.00686\cos(\delta) + 0.0157e_3\sin(\alpha) + 0.0972e_3\cos(\alpha)]10^{-10}\Delta\delta\Delta t^2 + [43.7]\Delta\alpha\Delta e_1 + [-331]\Delta\alpha\Delta e_2 + \\ & [83.2]\Delta\alpha^2\Delta e_1 + [-82.2]\Delta\delta^2\Delta e_1 + [165e_3\sin(\alpha) - 27.4e_3\cos(\alpha)]\Delta\alpha\Delta\delta + [-0.0972e_3\sin(\alpha)]10^{-10}\Delta\alpha\Delta\delta\Delta t^2 \end{aligned}$$

[1] J. Aasi et al. Einstein@Home all-sky search for periodic gravitational waves in LIGO S5 data. *Phys.Rev.*, D87(4):042001, 2013.

[2] J. Aasi et al. Application of a Hough search for continuous gravitational waves on data from the fifth LIGO science run. *Class.Quant.Grav.*, 31:085014, 2014.

[3] J. Aasi et al. Implementation of an F-statistic all-sky search for continuous gravitational waves in Virgo VSR1 data. *Class.Quant.Grav.*, 31:165014, 2014.

[4] J. Aasi et al. Searches for continuous gravitational waves from nine young supernova remnants. *ArXiv e-prints*, Dec. 2014.

[5] J. Aasi et al. A search of the orion spur for continuous gravitational waves using a "loosely coherent" algorithm on data from ligo interferometers. 93, 10 2015.

[6] J. Aasi et al. First low frequency all-sky search for continuous gravitational wave signals. *Phys. Rev. D*, 93:042007, Feb 2016.

[7] J. Aasi et al. Search of the Orion spur for continuous gravitational waves using a loosely coherent algorithm on data from LIGO interferometers. *Phys. Rev. D*, 93(4):042006, Feb. 2016.

[8] J. Abadie, B. P. Abbott, R. Abbott, T. D. Abbott, M. Abernathy, T. Accadia, F. Acernese, C. Adams, R. Adhikari, C. Affeldt, et al. All-sky search for periodic gravitational waves in the full S5 LIGO data. *Physical Review D*, 85(2):022001, 2012.

[9] J. Abadie et al. First search for gravitational waves from the youngest known neutron star. *Astrophys.J.*, 722:1504–1513, 2010.

[10] J. Abadie et al. All-sky Search for Periodic Gravitational Waves in the Full S5 LIGO Data. *Phys.Rev.*, D85:022001, 2012.

[11] B. Abbott et al. Setting upper limits on the strength of periodic gravitational waves from psr J1939 + 2134 using the first science data from the geo 600 and ligo detectors. *Phys. Rev. D*, 69:082004, Apr 2004.

[12] B. Abbott et al. Setting upper limits on the strength of periodic gravitational waves using the first science data from the GEO 600 and LIGO detectors. *Phys.Rev.*, D69:082004, 2004.

[13] B. Abbott et al. First all-sky upper limits from LIGO on the strength of periodic gravitational waves using the Hough transform. *Phys.Rev.*, D72:102004, 2005.

[14] B. Abbott et al. Limits on gravitational wave emission from selected pulsars using LIGO data. *Phys.Rev.Lett.*, 94:181103, 2005.

[15] B. Abbott et al. Coherent searches for periodic gravitational waves from unknown isolated sources and Scorpius X-1: Results from the second LIGO science run. *Phys.Rev.*, D76:082001, 2007.

[16] B. Abbott et al. Upper limits on gravitational wave emission from 78 radio pulsars. *Phys.Rev.*, D76:042001, 2007.

[17] B. Abbott et al. All-sky search for periodic gravitational waves in LIGO S4 data. *Phys.Rev.*, D77:022001, 2008.

[18] B. Abbott et al. Beating the spin-down limit on gravitational wave emission from the Crab pulsar. *Astrophys.J.*, 683:L45–L50, 2008.

[19] B. Abbott et al. All-sky LIGO Search for Periodic Gravitational Waves in the Early S5 Data. *Phys.Rev.Lett.*, 102:111102, 2009.

[20] B. Abbott et al. Einstein at Home search for periodic gravitational waves in early S5 LIGO data. *Phys.Rev.*, D80:042003, 2009.

[21] B. Abbott et al. The Einstein@Home search for periodic gravitational waves in LIGO S4 data. *Phys. Rev.*, D79:022001, 2009.

[22] B. Abbott et al. Searches for gravitational waves from known pulsars with S5 LIGO data. *Astrophys. J.*, 713:671–685, 2010.

[23] B. Abbott et al. Results of the deepest all-sky survey for continuous gravitational waves on LIGO S6 data running on the Einstein at Home volunteer distributed computing project. 2016.

[24] B. P. Abbott, R. Abbott, T. D. Abbott, M. R. Abernathy, F. Acernese, K. Ackley, C. Adams, T. Adams, P. Addesso, R. X. Adhikari, et al. Comprehensive all-sky search for periodic gravitational waves in the sixth science run LIGO data. *Physical Review D*, 94(4):042002, 2016.

[25] B. P. Abbott et al. All-sky search for periodic gravitational waves in LIGO S4 data. *Phys. Rev. D*, 77(2), 2008.

[26] B. P. Abbott et al. Comprehensive All-sky Search for Periodic Gravitational Waves in the Sixth Science Run LIGO Data. *ArXiv e-prints*, May 2016.

[27] B. P. Abbott et al. All-sky search for periodic gravitational waves in the o1 ligo data. *Phys. Rev. D*, 96:062002, Sep 2017.

[28] B. P. Abbott et al. All-sky search for periodic gravitational waves in the O1 LIGO data. *Phys. Rev. D*, 96:062002, Sep 2017.

[29] B. P. Abbott et al. Directional limits on persistent gravitational waves from advanced ligo’s first observing run. *Phys. Rev. Lett.*, 118:121102, Mar 2017.

[30] B. P. Abbott et al. First low-frequency einstein@home all-sky search for continuous gravitational waves in advanced ligo data. *Phys. Rev. D*, 96:122004, Dec 2017.

[31] B. P. Abbott et al. First search for gravitational waves from known pulsars with advanced LIGO. *The Astrophysical Journal*, 839(1):12, 2017.

[32] B. P. Abbott et al. Search for continuous gravitational waves from neutron stars in globular cluster ngc 6544. *Phys. Rev. D*, 95:082005, Apr 2017.

[33] V. Dergachev. On blind searches for noise dominated signals: a loosely coherent approach. *Class. Quantum Grav.*, 27(205017), 2010.

[34] V. Dergachev. Loosely coherent searches for sets of well-modeled signals. *Phys. Rev. D*, 85(062003), 2012.

[35] R. T. Edwards, G. B. Hobbs, and R. N. Manchester. www.atnf.csiro.au/research/pulsar/tempo.

[36] R. T. Edwards, G. B. Hobbs, and R. N. Manchester. tempo2, a new pulsar timing package – ii. the timing model and precision estimates. *Monthly Notices of the Royal Astronomical Society*, 372(4):1549–1574, 2006.

[37] A. L. Fey et al. The second realization of the international celestial reference frame by very long baseline interferometry. *The Astronomical Journal*, 150(58), August 2015.

[38] LIGO Scientific Collaboration. LIGO Analysis Library Suite.

[39] M. Pitkin, S. Doolan, L. McMenamin, and K. Wette. Reduced order modelling in searches for continuous gravitational waves – i. barycentring time delays. *Monthly Notices of the Royal Astronomical Society*, 476(4):4510–4519, 2018.

[40] A. Singh, M. A. Papa, H.-B. Eggenstein, S. Zhu, H. Pletsch, B. Allen, O. Bock, B. Maschenshalk, R. Prix, and X. Siemens. Results of an all-sky high-frequency einstein@home search for continuous gravitational waves in ligo’s fifth science run. *Phys. Rev. D*, 94:064061, Sep 2016.

[41] L. Wainstein and V. Zubakov. *Extraction of Signals from Noise*. 1971.